Vol 17 No 8, August 2008
1674-1056/2008/17(08)/2956-07

Chinese Physics B

© 2008 Chin. Phys. Soc.
and IOP Publishing Ltd

Fractal characteristics investigation on electromagnetic scattering from 2-D Weierstrass fractal dielectric rough surface*

Ren Xin-Cheng(任新成)[a)b)†] and Guo Li-Xin(郭立新)[a)]

[a)] *School of Science, Xi'dian University, Xi'an 710071, China*

[b)] *College of Physics and Electronic Information, Yan'an University, Yan'an 716000, China*

(Received 26 July 2007; revised manuscript received 25 March 2008)

A normalized two-dimensional band-limited Weierstrass fractal function is used for modelling the dielectric rough surface. An analytic solution of the scattered field is derived based on the Kirchhoff approximation. The variance of scattering intensity is presented to study the fractal characteristics through theoretical analysis and numerical calculations. The important conclusion is obtained that the diffracted envelope slopes of scattering pattern can be approximated as a slope of linear equation. This conclusion will be applicable for solving the inverse problem of reconstructing rough surface and remote sensing.

Keywords: dielectric rough surface, 2-D band-limited Weierstrass fractal function, fractal characteristics, Kirchhoff approximation

PACC: 4120, 4110H

1. Introduction

Since the fractal geometry was used as a new tool of describing naturally rough structures, many studies have been reported on the wave scattering from the fractal surface and various methods have been proposed in these studies.[1−17] Jaggard *et al*[18] proposed a 1-D band-limited Weierstrass function to model rough surface scattering and demonstrated that fractal surfaces permitted closed form expressions for the scattering coefficients under the Kirchhoff approximation, and the slope of the diffracted peak was 2.7 (2-D). Lin[19] extended the study to the case of 2D fractal surfaces, and discussed the influence of the surface fundamental wavenumber and fractal dimension on the pattern of the scattering field in the specular direction. Guo and Wu[20,21] studied fractal characteristics of electromagnetic scattering from a 2-D conducting rough surface, but they did not consider the case of dielectric rough surface. In this paper, a modified Weierstrass function is used to model a 2-D dielectric rough surface. A general solution for the variance of scattering intensity based on the Kirchhoff approximation is presented, and the important fractal information for bistatic scattering is obtained.

2. A 2-D Weierstrass fractal dielectric rough surface model and Kirchhoff approximation

A zero-mean modified 2-D band-limited Weierstrass function to model the rough surface is as follows:[20,21]

$$F(x,y)=\frac{\sqrt{2}\delta[1-b^{(2D-6)}]^{\frac{1}{2}}}{\left\{M[b^{(2D-6)N_1}-b^{(2D-6)(N_2+1)}]\right\}^{\frac{1}{2}}} \times\sum_{n=N_1}^{N_2} b^{(D-3)n}\sum_{m=1}^{M}\left\{\sin\left\{Kb^n\left[x\cos\left(\frac{2\pi m}{M}\right)+y\sin\left(\frac{2\pi m}{M}\right)\right]\right\}+\phi_{nm}\right\}, \quad (1)$$

*Project supported by the National Natural Science Foundation of China (Grant No 60571058), Specialized Research Fund for the Doctoral Program of Higher Education, China (Grant No 20070701010).

†E-mail: yauxchren@yahoo.com.cn

where δ is the root-mean-square (RMS) of the rough surface, D $(2 < D < 3)$ is the fractal dimension, K is the fundamental wavenumber, b is the fundamental spatial frequency, N and M are the numbers of tons, and ϕ_{nm} is a phase term that has a uniform distribution over the interval $[-\pi, \pi]$. This function shows a combination of both deterministic periodic structure and random rough structure. As a model for physical fractals, this function is also excellent, for it possesses a very large derivative and a finite band of special frequency and exhibits being self-affine over a corresponding finite range of resolution. It is a multi-scale surface with the same roughnesses down to some fine scales. Since natural surfaces are generally neither purely random nor purely periodic, but often anisotropic, the above proposed function is a good candidate for modelling natural surfaces.

Consider an incident wave impinging on the 2-D dielectric surface characterized by the above fractal function $F(x, y)$ extending from $x = -L_x$ to L_x, $y = -L_y$ to L_y, as shown in Fig.1.

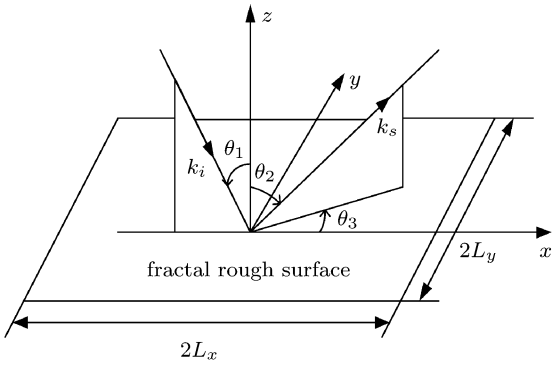


Fig.1. Geometry of scattering from the two-dimensional fractal rough surface.

Here, we use the Kirchhoff approximation to study the scattering from a rough surface that takes the exact roughness profiles into account. A small angle interaction will be used to avoid the problem of shadowing (i.e. neglecting the edge effect). If the observation is performed at the far field of the scattered wave, the scattered field under the Kirchhoff approximation can be given by[22−24]

$$\psi_{\rm sca}(\boldsymbol{r}) = -\frac{{\rm i}k\exp({\rm i}kr)}{4\pi r}2\xi(\theta_1,\theta_2,\theta_3) \times \int_{-L_x}^{L_x}\int_{-L_y}^{L_y}\exp[{\rm i}k\phi(x',y')]{\rm d}x'{\rm d}y' + \psi_{\rm e}, \tag{2}$$

$$\xi(\theta_1,\theta_2,\theta_3) = \frac{1}{2}\left(\frac{AA'}{C} + \frac{BB'}{C} + D\right), \tag{3}$$

$$\phi(x',y') = Ax' + By' + CF(x',y'), \tag{4}$$

$$A = \sin\theta_1 + \sin\theta_2\cos\theta_3, \tag{5}$$

$$B = -\sin\theta_2\sin\theta_3, \tag{6}$$

$$C = -(\cos\theta_1 + \cos\theta_2), \tag{7}$$

$$A' = R(\sin\theta_1 - \sin\theta_2\cos\theta_3), \tag{8}$$

$$B' = R\sin\theta_2\sin\theta_3, \tag{9}$$

$$D = R(\cos\theta_1 + \cos\theta_2), \tag{10}$$

and

$$\psi_{\rm e} = -\frac{{\rm i}k\exp({\rm i}kr)}{4\pi r}\left\{\frac{{\rm i}A'}{kD}\int_{-L_y}^{L_y}[\exp{\rm i}k\phi(L_x,y') - \exp{\rm i}k\phi(-L_x,y')]{\rm d}y' + \frac{{\rm i}B'}{kD}\int_{-L_x}^{L_x}[\exp[{\rm i}k\phi(x',L_y)] - \exp[{\rm i}k\phi(x',-L_y)]{\rm d}x'\right\}, \tag{11}$$

where the function $\psi_{\rm sca}(\boldsymbol{r})$ denotes the scattering field; r is a distance from the origin to a point of the scattering field; k is the incident module defined as $k = 2\pi/\lambda$ with λ being the incident wavelength; the term $\psi_{\rm e}$ is related to the edge effect; R is the Fresnel reflection coefficient of the tangential plane at the point of interest, that is

$$R_{\rm h} = \frac{\cos\theta_1 - \sqrt{\varepsilon - \sin^2\theta_1}}{\cos\theta_1 + \sqrt{\varepsilon - \sin^2\theta_1}}$$

and

$$R_{\rm v} = \frac{\varepsilon\cos\theta_1 - \sqrt{\varepsilon - \sin^2\theta_1}}{\varepsilon\cos\theta_1 + \sqrt{\varepsilon - \sin^2\theta_1}} \tag{12}$$

with $R_{\rm h}$ and $R_{\rm v}$ denoting the horizontal polarization and the vertical polarization to the incident plane wave, respectively.

A more appropriate quantity for analysing the properties of the average scattering field is $\bar{\psi}_{\rm sca}(\boldsymbol{r})$ defined as

$$\bar{\psi}_{\rm sca}(\boldsymbol{r}) = \langle\psi_{\rm sca}(\boldsymbol{r})\rangle_{\phi_{nm}}. \tag{13}$$

From expression (2), we obtain

$$\bar{\psi}_{\rm sca}({\rm r}) = -\frac{{\rm i}kL_xL_y{\rm e}^{-{\rm i}kr}}{\pi r}2\xi(\theta_1,\theta_2,\theta_3)\left[\prod_{n=N_1}^{N_2} J_0^M(C_k b^{(D-3)n})\right]\cdot \sin c(kAL_x)\cdot \sin c(kBL_y)+\psi_{\rm e}, \tag{14}$$

where $\sin c(x) = \sin(x)/x$, and the coefficient

$$C_k = -2k\delta\cos\theta_1\left[\frac{2(1-b^{2(D-3)})}{(b^{2(D-3)N_1}-b^{2(D-3)(N_2+1)})M}\right]^{\frac{1}{2}}. \tag{15}$$

The edge effect term can be written as

$$\psi_{\rm e} = -\frac{{\rm i}k{\rm exp}({\rm i}kr)}{\pi r}\left(\frac{AA'+BB'}{C}\right)\lim_{x\to\pm L_x} x\sin c(kAx)\lim_{y\to\pm L_y}\sin c(kBy). \tag{16}$$

From the above expressions, a statistical parameter of the scattering field named the variance of scattering intensity, $\sigma_{\rm I}$, can be written as

$$\begin{aligned}\sigma_{\rm I} =& \frac{\bar{I}(\boldsymbol{r})-\bar{\psi}^2_{\rm sca}(\boldsymbol{r})}{I_0}\\ =& \frac{\langle\psi_{\rm sca}(\boldsymbol{r})\psi^*_{\rm sca}(\boldsymbol{r})\rangle_{\phi_{nm}}-\langle\psi_{\rm sca}(\boldsymbol{r})\rangle_{\phi_{nm}}\langle\psi_{\rm sca}(\boldsymbol{r})\rangle^*_{\rm sca}}{\psi_{\rm sca0}(\boldsymbol{r})\psi^*_{\rm sca0}(\boldsymbol{r})}\\ =& \frac{\xi^2(\theta_1,\theta_2,\theta_3)C_k^2}{4\cos^2\theta_1}\sum_{n=N_1}^{N_2}\sum_{m=1}^{M} b^{2(D-3)n}\sin c^2\left[\left(kA+Kb^n\cos\frac{2\pi m}{M}\right)L_x\right]\sin c^2\left[\left(kB+Kb^n\sin\frac{2\pi m}{M}\right)L_y\right].\end{aligned} \tag{17}$$

$\psi_{\rm sca0}(\boldsymbol{r})$ in expression (17) is the scattering field in the specular direction ($\theta_1 = \theta_2$ and $\theta_3 = 0$) from a perfectly smooth surface which can be derived from expression (2). We consider the scattering from a dielectric rough surface as a suitable approximation to many naturally occurring surfaces. In this case, the Fresnel reflection coefficient is expressed as expression (12). Here the variance of scattering intensity, $\sigma_{\rm I}$, can be used to study the diffraction away from the specular direction and to determine the influence of fractal dimension on the pattern of scattering field. The advantage of this representation is that only the average effects of intensity and scattering field need considering. Thus we need not measure the phase terms of the scattering wave which are difficult to extract.

3. Fractal characteristic investigation

First, the average scattered intensities are computed, and the scattered intensities in the specular direction have almost identical values for the same values of δ at the same incident angles and wave lengths. With the increase of isotropy of the surfaces, more scatterings occur in the off-specular direction. Scattering in the specular direction is more useful for determining the influence of fractal parameters on the pattern of scattered field.

Second, the variance of scattering intensity, $\sigma_{\rm I}$, from this kind of fractal surface is calculated from expression (17). We use this second moment of the scattering field to study the diffraction pattern away from the specular direction. In Fig.2 the variations of $\sigma_{\rm I}$ with $\theta(\theta_1 = \theta_2 = \theta$, and $\theta_3 = \pi)$ (i.e. backscattering) are shown for different patch sizes, where the incident wave is the horizontal polarization plane wave, the parameters are $N_1 = 0, N_2 = 9$, $b = 1.6$, $D = 2.67$, $\delta = 0.05\lambda, \lambda = 0.003m$ (It is not announced in hereinafter), and the permittivity of dielectric $\varepsilon = 48 - j34$. In fact, the variance of the scattering pattern with different surface patch sizes is of interest in remote sensing. If we increase the patch sizes for both L_x and L_y, more information will be detected. If these sizes are small than some periods of the surfaces, some scattering information will be lost (Fig.2(a)). It should be noted that the edge effects, which are not taken into account, are not negligible for small patch sizes, which means that the patch size we choose must be large enough for us to examine this fractal surface. In fact, if the patch size is greater than $K/2\pi$ (fundamental period) (Fig.2(b)), then the scattering pattern will have no change qualitatively.

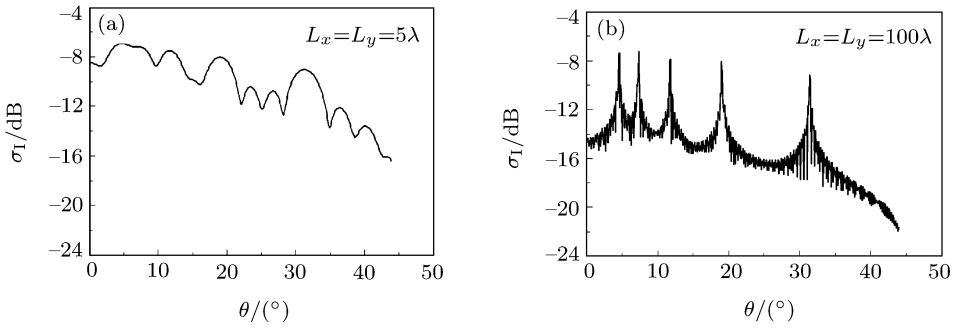


Fig.2. Variations of σ_I with θ for different patch sizes.

The parameter K in expression (1) is defined as the fundamental wavenumber of the fractal surface, and $K/2\pi$ represents the largest wavelength of the tested surface. In Fig.3, σ_I is presented as a function of θ with different wavenumbers. For $K\lambda < 0.01$, the high frequency components away from the specular direction will concentrate in the specular direction. For this kind of surface, intensities away from the specular direction monotonically decays rapidly. For $K\lambda > 10$, the scattering field will be close to that from a perfectly smooth surface, and the RMS of the scattered field becomes very small, which means that this surface can be treated as a smooth surface, for the largest wavelength is smaller than the incident wavelength. The incident wave length can be viewed as a yardstick to probe rough surface. For $0.01 < K\lambda < 10$, more high frequency components appear in the off-specular direction. This kind of surface is more interesting, for the decay of high frequency components can be used to analyse the influence of surface parameters in the scattered field.

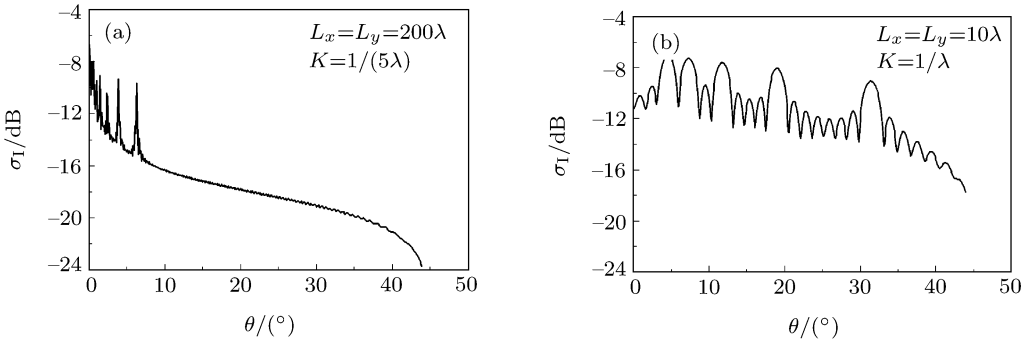


Fig.3. Variations of σ_I with θ for different fundamental wavenumbers.

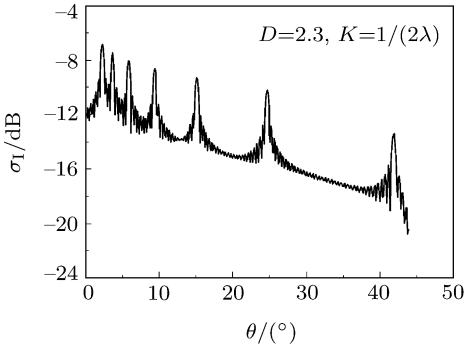


Fig.4. Variation of σ_I with θ in the backscattering.

Third, we numerically calculate σ_I for the backscattering. In Fig.4, the back scattering variation of σ_I is shown for the case of $K = 1/(2\lambda)$, and $D = 2.3$. The relationship between the diffracted envelope slopes and D with different values of K does not satisfy the linear equation through plentiful calculations. It is not similar to the case of conducting rough surface.[6,7]

Finally, we also numerically calculate the values of σ_I for different values of fractal dimensional D with the emphasis on the studying of the scattering pattern and fractal dimension for bistatic scattering. With the increase of fractal dimension D, diffraction of lower frequency components away from the specular direc-

tion in the scattering field is suppressed but that of high frequency components is enhanced. Decay of diffraction away from the specular direction is not linearly decreasing with D, especially when D is close to 2.95. Examples for different values of fractal D are illustrated in Fig.5.

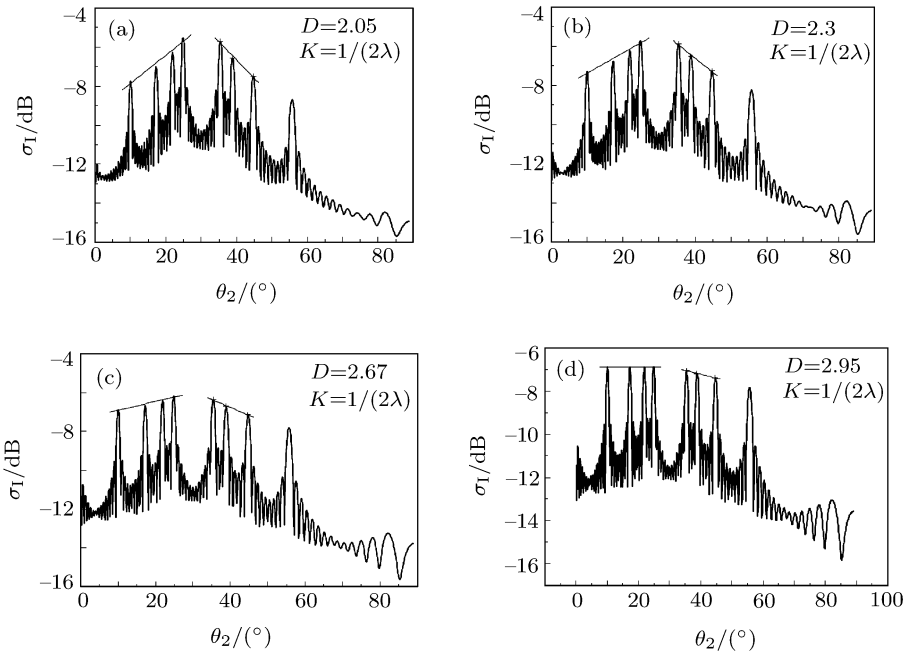


Fig.5. Variations of $\sigma_{\rm I}$ with θ_2 for different values of D.

It is obvious that the patterns of $\sigma_{\rm I}$ seem to be similar to each other, with the values of K and b being finite for different values of D, but the envelope slopes of the scattering pattern are somewhat different. The bigger the value of D is, the smaller the slope will be. This result can be interpreted by the Bragg match condition or the conservation of momenta[12] that higher fractal dimensions tend to provide equal-strength coupling of various spatial frequencies, while lower fractal dimensions will give higher strength to the coupling near the specular reflection. This tendency implies that the fractal dimension of the scattering rough surface can be estimated from its scattering pattern. In order to examine the relation between fractal dimension and scattering pattern, the envelope slopes of scattering pattern for different values of D and K can also be obtained as shown in Fig.6.

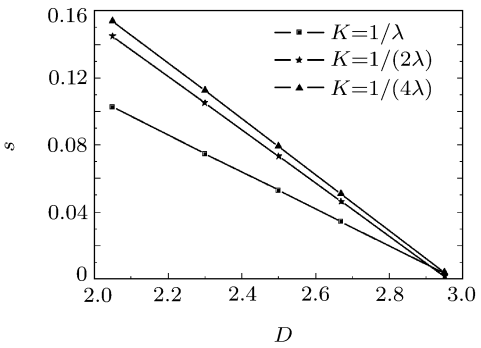


Fig.6. The envelope of scattering pattern versus fractal dimension D.

We are glad to see that the scattering pattern in the near forward direction can be approximated as a slope of linear equation which can be written as (for $K=\dfrac{1}{\lambda}, \dfrac{1}{2\lambda}, \dfrac{1}{4\lambda}$, respectively)

$$s = 0.32782 - 0.11000D \approx 0.11000(3-D),$$
$$s = 0.47138 - 0.15925D \approx 0.15925(3-D),$$

and

$$s = 0.49466 - 0.16629D \approx 0.16629(3-D). \quad (18)$$

It is easily concluded from expression (18) that the relationship between the envelope slope and D could be given as

$$s = A_1(K) * (3 - D), \tag{19}$$

where $A(K)$ is a constant with K varying.

We are also glad to see that the scattering pattern in the right of specular direction but near the specular direction can be approximated as a slope of linear equation which can be written as (for $K = \frac{1}{\lambda}, \frac{1}{2\lambda}, \frac{1}{4\lambda}$, respectively)

$$s = 0.11436D - 0.34407 \approx 0.11436(D - 3),$$
$$s = 0.17126D - 0.54070 \approx 0.17126(D - 3),$$

and

$$s = 0.26569D - 0.82222 \approx 0.26569(D - 3). \tag{20}$$

It is easy to conclude from expression (20) that the relationship between the envelope slope and D could be given as

$$s = A_2(K) * (D - 3), \tag{21}$$

where $A(K)$ is a constant with K varying. Expressions (18) and (19) are the most important results we have obtained in this paper, and these results will be applicable for solving the inverse problem of reconstructing rough surface and remote sensing.

Compared with the case of conducting rough surface, the shape of curve i.e. the variation of σ_{I} with θ (backscattering) or θ_2 (bistatic scattering) is similar under the condition that the other parameters are the same, and the curve moves airward only, this is comprehended easily. As an example, Fig.7 shows this instance.

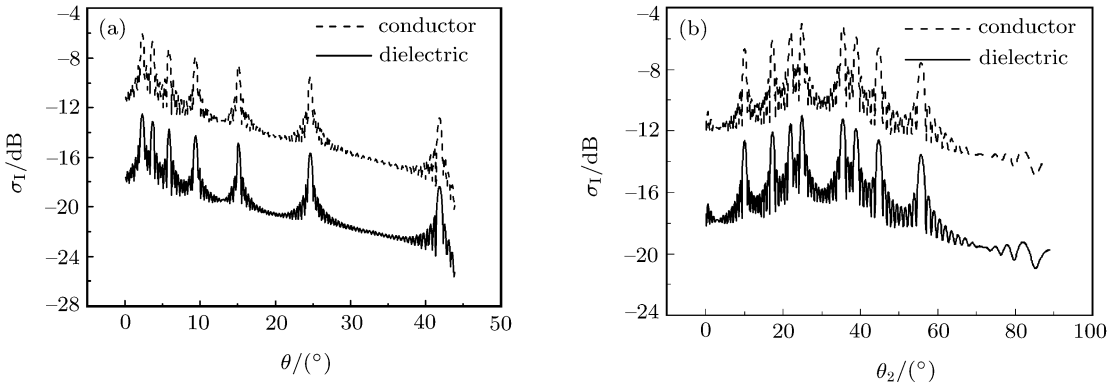


Fig.7. Comparisons between conductor and dielectric in backscattering (a) and bistatic scattering (b).

Some general conclusions are obtained for backscattering and bistatic scattering through plentiful calculations. For example, for two kinds of dielectric materials, of which the permittivities are real, the shapes of curve i.e. the variations of σ_{I} with θ (backscattering) or θ_2 (bistatic scattering) are similar under the conditions that the other parameters are the same, the curve corresponding to the dielectric of bigger permittivity moves up, whereas, the curve corresponding to the dielectric of smaller permittivity moves down.

We study the case in which the incidence wave is the horizontal polarization wave hereinbefore, these results are appropriate to the case in which the incidence wave is the vertical polarization wave by analysing expressions (12) and (17) and plentiful calculation.

4. Conclusions

In this paper, a modified fractal Weierstrass function is used to model a two-dimensional fractal rough surface, and a general solution for the scattered field based on the Kirchhoff approximation is given to dielectric rough surface. The influence of fractal dimension, the patch size of surface and the fundamental wavenumber on the scattering field is discussed theoretically and numerically. The important fractal information on scattering pattern in the near forward direction and in the right of specular direction near the specular direction is obtained. These results will be applicable for solving the inverse problem of reconstructing rough surface and remote sensing.

References

[1] Mandelbrot B B 1983 *The Fractal Geometry of Nature* (San Francisco: Freeman)

[2] Guo L X and Wu Z S 2001 *J. Chin. Phys. Lett.* **18** 42

[3] Guo L X and Wu Z S 2002 *J. Electric & Information Technology.* **24** 1405 (in Chinese)

[4] Guo L X, Ren Y C and Wu Z S 2005 *J. Electric & Information Technology.* **27** 1666 (in Chinese)

[5] Guo L X and Wei G H 2005 *Commun. Theor. Phys.* **44** 90

[6] Wang Y H, Guo L X and Wu Q 2006 *Chin. Phys.* **15** 1755

[7] Liu Y, Wei E B, Hong J L and Ge Y 2006 *Chin. Phys. Soc.* **15** 2175

[8] Guo L X, Wang Y H and Wu Z S 2005 *Acta Phys. Sin.* **54** 96 (in Chinese)

[9] Yang J L, Guo L X and Wan J W 2005 *Acta Phys. Sin.* **54** 2106 (in Chinese)

[10] Guo L X, Wang Y H and Wu Z S 2005 *Acta Phys. Sin.* **54** 5130 (in Chinese)

[11] Wang Y H, Guo L X and Wu Z S 2006 *Acta Phys. Sin.* **55** 5191 (in Chinese)

[12] Guo L X, Wang Y H and Wu Z S 2006 *Acta Phys. Sin.* **55** 5815 (in Chinese)

[13] Wang Y H, Guo L X and Wu Z S 2007 *Acta Phys. Sin.* **56** 0186 (in Chinese)

[14] Huang J Y and Li Y L 2006 *Chin. Phys. Soc.* **15** 281

[15] Sun X H, Xiao J B and Zhang M D 2006 *Chin. Phys. Soc.* **15** 143

[16] Dai S Y, Wu Z S and Xu Y B 2007 *Acta Phys. Sin.* **56** 786 (in Chinese)

[17] Li M Q, Tao X J and Wu X L 2007 *Acta Phys. Sin.* **56** 2115 (in Chinese)

[18] Jaggard D L and Kim Y 1987 *J. Opt. Soc. Am.* A **7** 1131

[19] Lin N 1995 *J. Mod. Opt.* **42** 225

[20] Guo L X, Wu Z S and Ke X Z 2000 *J. Acta Electronic Sin.* **28** 128

[21] Guo L X and Wu Z S 2000 *J Acta Phys. Sin.* **49** 1064

[22] Ogilvy J A 1991 *Theory of Wave Scattering from Random Rough Surface* (Bristol: Institute of Physics Publishing) p39

[23] Fung A K 1994 *Microwave Scattering and Emission Models and Their Applications* (London: Artech House) p163

[24] Ulaby F T, Moore R K and Fung A K 1982 *Microwave Remote Sensing* Vol.II (London: Addision-Wesley) p816